

# How Heavy Is It? Humanoid Robot Estimating Physical Properties of Unknown Objects Without Force/Torque Sensors

Zizhou Lao<sup>1</sup>, Yuanfeng Han<sup>2</sup> and Gregory S. Chirikjian<sup>1,2</sup>

**Abstract**—Many robots utilize commercial force/torque sensors to identify physical properties of a priori unknown objects. However, such sensors can be difficult to apply to smaller-sized robots due to their weight, size, and high-cost. In this paper, we propose a framework for smaller-sized humanoid robots to estimate the inertial properties of unknown objects without using force/torque sensors. In our framework, a neural network is designed and trained to predict joint torque outputs. The neural network’s inputs are robot’s joint angle, steady-state joint error, and motor current. All of these can be easily obtained from many existing smaller-sized robots. As the joint rotation direction is taken into account, the neural network can be trained with a smaller sample size, but still maintains accurate torque estimation capability. Eventually, the inertial properties of the objects are identified using a nonlinear optimization method. Our proposed framework has been demonstrated on a NAO humanoid robot.

## I. INTRODUCTION

In order to manipulate different daily objects, it is crucial for humanoid robots to identify inertial properties of those objects. This process usually requires a humanoid robot to continuously interact with an object and then estimate its inertial properties based on the information of the sensors equipped on that robot.

Many existing methods for object physical property identification are based on the measurements using commercial force/torque (F/T) sensors. For example, a dynamic estimation of physical properties using end-effector wrench during general manipulator movement is proposed in [1]. The mass and center of mass (CoM) of an object is estimated by tipping and leaning operations [2]. [3] and [4] propose methods focusing on the estimation of CoM of an object in planar motions. A similar problem is considered in [5] to identify the physical properties of unknown objects by planning planar pushing motions. In [6], the physical properties of unknown boxes are identified by a force sensing plate attached to the feet of a humanoid robot.

Since commercial F/T sensors are often heavy and expensive, they are not commonly equipped on smaller-sized humanoid robots. Therefore, it is still challenging for smaller-sized humanoid robots to estimate inertial properties such as mass and center of mass (CoM) location of unknown objects [7], [8], [9]. Despite lacking direct F/T sensing ability, many smaller-sized robots possess other sensors mounted on each

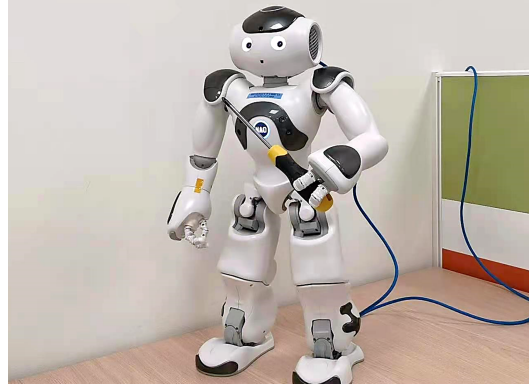


Fig. 1. The NAO is estimating the inertial properties of an unknown screwdriver.

joint, such as encoders and electric current sensors [10], [11], [12]. Although such sensors may be noisy in nature, they incorporate information for robot’s joint torques, which directly relate to the inertial properties of the object that the robot grips. Here, we are specifically interested in estimating object inertial properties with existing sensors on smaller-sized humanoid robots.

Similar to object inertial property identification, another relevant field of research is robot interaction force or joint torque reconstruction. Many of these works do not use F/T sensors to construct interaction forces. In [13] and [14], neural networks are used to map the relationship between joint torques without external forces and joint motions. In [15], the authors investigate the effects of tool data and video sequences on force estimation for surgical robots and design convolutional neural networks to estimate interaction forces. In [16], joint steady-state control error is utilized to reconstruct interaction forces analytically for a humanoid robot. There are also many works using neural networks to infer interaction forces from visual data [17] or video [18].

On the one hand, some of above-mentioned works directly model joint torques as proportional to the electric currents of the motors. The noisy nature of the electric current is ignored which can result in poor estimation performance. On the other hand, the frictional torques are often ignored in the afore mentioned approaches, which can not be simply calculated analytically. In addition, many vision based methods require complex system setup, which is difficult to be widely applied to various robots.

In this paper, we propose a framework for a smaller-sized humanoid robot to identify the mass and CoM location of a priori unknown objects without using F/T sensors. A

<sup>1</sup>Department of Mechanical Engineering, National University of Singapore, Singapore lao.zizhou@nus.edu.sg, mpegre@nus.edu.sg

<sup>2</sup>Laboratory for Computational Sensing and Robotics, Johns Hopkins University, Baltimore, MD, USA yhan33@jhu.edu, gchirik1@jhu.edu

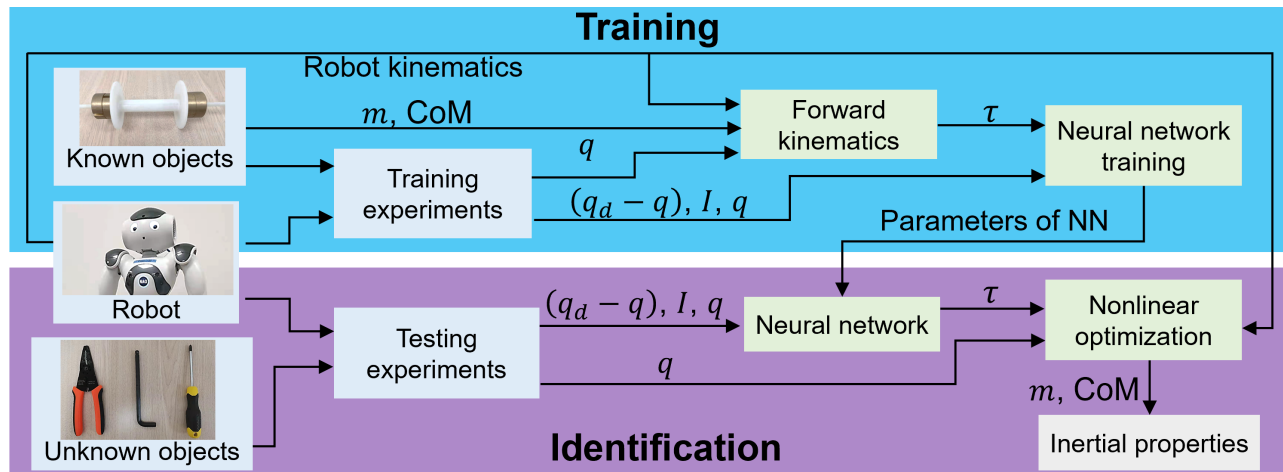


Fig. 2. Block diagram for the neural network training process (top, blue) and the object inertial property identification process (bottom, purple).

neural network is first designed to estimate joint torques. The network inputs include motor electric current, joint angle and steady-state joint angle error, which can be measured by encoders and current sensors commonly existing in many smaller-sized robots. In the training process, the robot grips an object with known mass and CoM location to reach different configurations. In each configuration, the modelled joint torques can be derived analytically based on the known end-effector wrenches and are later used as labels for the neural network training.

In the object inertial property identification process, the robot first tests the object in different configurations and reaches different configurations. Then a nonlinear optimization technique is implemented to search for a set of optimal inertial parameters of the objects, of which the modelled torques best match the estimated torques from the neural network.

For both training and identification processes, we take the direction of frictional torque into account and design the training and identification trajectories such that the joints always do positive work (see Section III-C) when approaching the desired configurations. This method reduces the sample size for the network training process, but still enables accurate joint torque estimation capability of the network.

The proposed method is demonstrated on a NAO humanoid robot. (Fig. 1). Six a priori unknown objects are used to evaluate the method's performance. Results show that our proposed method is able to provide relatively accurate estimation results of the masses and CoM locations of those testing objects.

## II. METHOD OVERVIEW

Our proposed approach includes two steps: **training** and **identification**. The block diagram is shown in Fig. 2.

In the **training** step, a neural network is used to estimate joint torque taking joint electric current, joint angle steady-state error and joint angle as inputs. The sensor outputs of several with a priori known inertial properties are collected

during training process. The modelled joint torques are derived analytically by forward kinematics of the robot, which are used as labels of the training data. Then the network is trained by inputs and labels.

In the **identification** step, the robot grips an unknown object and tests it in different arm configurations. Then a nonlinear optimization approach is applied to search a set of optimal inertial parameters of the object to match the estimated joint torque from neural network and the modelled joint torque.

A NAO robot is used as our testing platform. Each arm of the robot includes five joints: ShoulderPitch, ShoulderRoll, ElbowYaw, ElbowRoll and WristYaw. Since the moment arm between the wrist and the hand gripping position of the robot is very short, the wrist torque barely change in different arm configurations. In addition, the shoulder motors of the robot are much weaker compared with elbow joints, which limit their capacities of motion in different arm configurations. As a result, the ElbowYaw and ElbowRoll joints are used in our training and identification steps.

Considering that the static joint torque is affected by the direction of rotation, a planning strategy is developed. This planning method significantly reduces the training sample numbers which prevent the motor of the robot from over-heat from long-term experiments, but still enable accurate identification results.

## III. NEURAL NETWORK TRAINING

### A. Neural Network Input

The joint electric current, joint angle steady-state error and joint angle are chosen as inputs for the neural network.

**Joint electric current:** In theory, the magnitude of measured joint torque  $\tau_m$  can be directly calculated from the electric current  $I$  of the joint motor:  $\tau_m = IK_a K_b$ , in which  $K_a$  and  $K_b$  are the motor constant and the motor reduction ratio. However, electric current alone does not infer the torque direction and it is usually too noisy to be used to measure accurate joint torques. Another shortcoming is the lack of consideration of friction.

**Joint angle steady-state error:** PD control has been adopted by many robots as their joint control strategy [16], [19], [20]. The joint angle steady-state error from such controller can directly determine both the magnitude and the direction of the joint torque  $\tau_m$ :  $\tau_m = (q_d - q)K_p R K_a K_b$ , in which  $q_d$  and  $q$  are the command joint angle value and the measured joint angle value by an encoder.  $K_p$  is the proportional controller gain and  $R$  is a constant between motor current and controller output.

**Joint angle:** Static friction generates measurement error for joint torque estimation for both the above-mentioned methods. Considering the static friction can be influenced by the joint configuration, the joint angle ( $q$ ) is also included as an input for the neural network.

### B. Robot Arm Motion Planning

For each training object, the moving ranges of ElbowYaw and ElbowRoll joints are between  $-80^\circ \sim -20^\circ$  and  $-70^\circ \sim -20^\circ$ . The configurations for both joints are uniformly distributed with  $10^\circ$  intervals and the training configuration space is shown as blue circles in Fig. 3(a), left. The sensor data from overall 42 different configurations are collected.

A smooth trajectory which connects all the nodes in the configuration space is constructed for the training process. Initially, the configuration which is the lowest in the Cartesian space is chosen as a starting node of the trajectory. Afterwards, an iterative process takes place which connects the previous node to its nearest unvisited node in the Cartesian space. This process ends when all the nodes in the configuration space are connected. The planned trajectory is shown in Fig. 3(a), right.

### C. Joint Moving Direction Control

We define **effective joint torque** ( $\tau$ ) as the torque exerted on joints due to all the external forces acting on robots (including own weights of robots). When a robot reach steady state, the **motor torque** ( $\tau_m$ ) should be balanced by the summation of effective joint torque and **frictional torque** ( $\tau_f$ ). The purpose of the neural network in this paper is to eliminate frictional torque and estimate effective joint torque accurately.

The magnitude of joint motor torque at steady state can be significantly affected by the moving direction (clockwise or counter-clockwise) in which the joint rotates to its final state. Two possible conditions need to be considered. Given an example of arm link rotating around a fixed axis, if the arm link reaches its steady state along a counter-clockwise direction (Fig. 3(b), left), the frictional torque  $\tau_f$  is in clockwise direction to oppose the motion. In this case, the motor torque  $\tau_m$  does positive work while the effective joint torque  $\tau$  does negative work and  $\tau_m = \tau + \tau_f$ . When the arm link reaches its steady state along a clockwise direction, the motor torque does negative work while the effective joint torque does positive work and  $\tau_m = \tau - \tau_f$ , as shown in Fig. 3(b), right. The above-mentioned two conditions lead to different joint angle steady-state errors and joint currents.

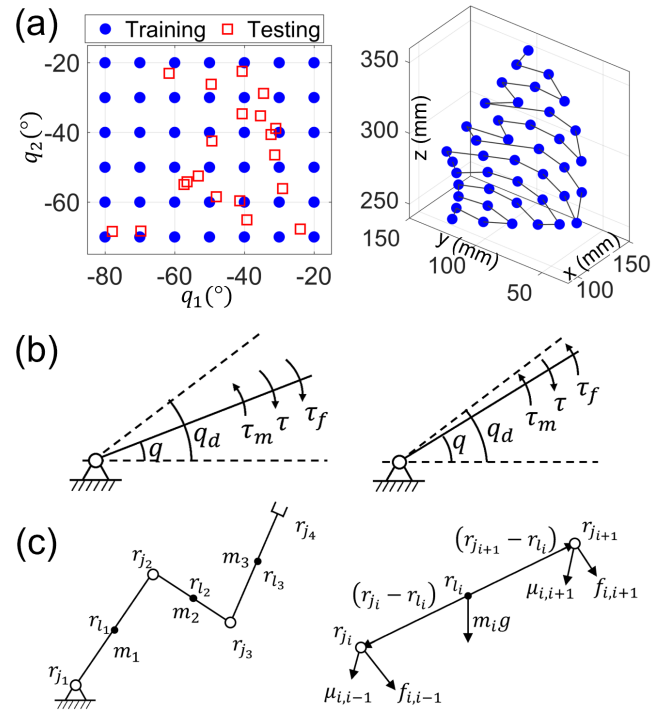


Fig. 3. (a) Left: Training (blue circle) and testing (red square) elbow joint configurations for the neural network. Right: Planned trajectory for connecting training joint configurations visualized in Cartesian space. (b) Friction effect on joint torque. Left: Counter-clockwise motion. Right: Clockwise motion. (c) Analytical derivation of joint torque with known objects. Left: An example of a robot. Right: Free body diagram of  $i$ -th link.

**Positive-work direction** of a joint is defined as the rotational direction along which motor torque  $\tau_m$  does positive work. Positive-work direction can be determined as the opposite direction of effective joint torque  $\tau$ . Regarding the example in Fig. 3(b), left, the joint is rotating along positive-work direction to reach steady state.

To simplify the training process, the robot arm is controlled to only move along the positive-work direction (This is also applied to the testing process). Since the inertial properties of the objects are known in training process, the joint torques can be solved analytically for each configuration (see Section III-D). Then the positive-work directions for each controlled joint can be subsequently acquired. In practice, the robot first moves to a generated prior configuration before moving to each node in the designed configuration space (Fig. 3(a), left), such that the joint always reaches to its desired configuration along a positive-work direction. Prior configuration is generated by rotate each joint along the opposite positive-work direction for a certain angle.

### D. Modelled Torque Derivation

The modelled joint torque based on the inertial properties of the training objects are used as labels for the neural network. Given a serial robot with  $n$  links and  $n$  joints as shown in Fig. 3(c), left, the coordinates of joints  $r_{j_i}$  ( $i = 1, \dots, n$ ), end-effector  $r_{j_{n+1}}$  and CoMs of links  $r_{l_i}$  ( $i = 1, \dots, n$ ) can be derived from kinematics. The free body diagram of  $i$ -th link is shown in Fig. 3(c), right.  $f_{i,i+1}$  and

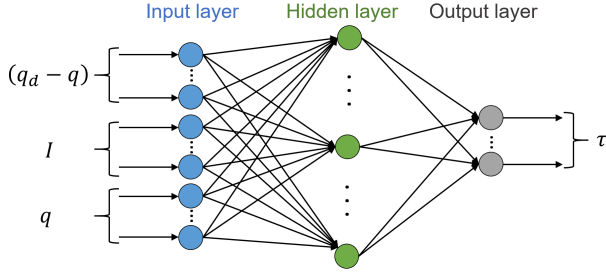


Fig. 4. Neural network for effective joint torque estimation.

$\mu_{i,i+1}$  are the force and moment applied on  $i$ -th link by  $(i+1)$ -th link. Similarly,  $f_{i,i-1}$  and  $\mu_{i,i-1}$  are the force and moment applied on  $i$ -th link by  $(i-1)$ -th link. When the robot is in stationary, the following equations can be built from Newton's Laws.

$$f_{i,i+1} + m_i g + f_{i,i-1} = 0 \quad (1)$$

$$(r_{j_{i+1}} - r_{l_i}) \times f_{i,i+1} + \mu_{i,i+1} + (r_{j_i} - r_{l_i}) \times f_{i,i-1} + \mu_{i,i-1} = 0 \quad (2)$$

where  $m_i$  is the mass of  $i$ -th link. Eq. 1 refers to the forces exerted on the link. Eq. 2 refers to the resultant moment around the CoM of the link.

The forces and moments between two adjacent links are equal in magnitude but opposite in direction, i.e.

$$f_{i,i+1} = -f_{i+1,i} \quad (3)$$

$$\mu_{i,i+1} = -\mu_{i+1,i}. \quad (4)$$

Given external force and moment applied on end-effector, the forces and moments on all the joints from end-effector to the base can be solved recursively.

The joint torque on a certain joint applied by motor is the component of moment along the direction of rotational axis. Given the unit vector  $z_i$  along rotation axis of joint  $i$ , the joint torque can be solved as

$$\tau_i = \mu_{i,i-1} \cdot z_i. \quad (5)$$

#### E. Neural Network Details

A multilayer perceptron (MLP) is used as the structure of the neural network (Fig. 4). For each set of data, the input of the network is a 28-dimensional vector, consisting of joint angle error of elbow joints (2 dimensions), currents of elbow joints (2 dimensions) and joint angle of robot (24 dimensions). The effective joint torques (see Section III-C) of elbow joints (2-dimensional vector) are the output of the network. In summary, the neural network is a 28 – 50 – 2 MLP, with ReLU as activation function in hidden layer. This trained network aims to provide estimation for the effective torque using the robot's sensor data.

#### IV. OBJECT INERTIAL PROPERTY IDENTIFICATION

A nonlinear optimization technique is adopted for identifying the mass and CoM location of an a priori unknown object. In practice, the robot holds the object and reaches 20 different arm configurations. The estimated effective torques

---

#### Algorithm 1 Positive-work Direction Detection

---

```

Move to desired configuration  $q_d$ 
Joint Index  $i \leftarrow 1$ 
while  $i \leq N$  do
  (For positive direction)
  Rotate joint  $i$  from  $(q_d)_i$  to  $(q_d)_i - \Delta q$ 
  Sleep for time  $\Delta t$ 
  Rotate joint  $i$  from  $(q_d)_i - \Delta q$  to  $(q_d)_i$ 
  Sleep for time  $\Delta t$ 
  Collect joint angle error  $e_{i,pos} = (q_d)_i - q$ 
  (For negative direction)
  Rotate joint  $i$  from  $(q_d)_i$  to  $(q_d)_i + \Delta q$ 
  Sleep for time  $\Delta t$ 
  Rotate joint  $i$  from  $(q_d)_i + \Delta q$  to  $(q_d)_i$ 
  Sleep for time  $\Delta t$ 
  Collect joint angle error  $e_{i,neg} = (q_d)_i - q$ 
  if  $|e_{i,pos}| \geq |e_{i,neg}|$  then
    Mark flag for joint  $i$  as  $F_i = 1$ 
  else if  $|e_{i,pos}| < |e_{i,neg}|$  then
    Mark flag for joint  $i$  as  $F_i = -1$ 
  end if
   $i = i + 1$ 
end while

```

---

$\tau_i = [\tau_i^1, \tau_i^2] \in \mathbb{R}^2$  can be obtained from the trained neural network. The effective joint torques can also be formulated as a function related to the inertial properties of the unknown object and the configuration of the robot  $\mathbf{q}$ :

$$\begin{bmatrix} \tau_1 \\ \tau_2 \\ \vdots \\ \tau_n \end{bmatrix} = \begin{bmatrix} f(\mathbf{CoM}, m, \mathbf{q}_1) \\ f(\mathbf{CoM}, m, \mathbf{q}_2) \\ \vdots \\ f(\mathbf{CoM}, m, \mathbf{q}_n) \end{bmatrix} \quad (6)$$

Here we try to search the optimal value of  $\mathbf{CoM}^*$  and  $m^*$  which best fit the modelled joint torque to the estimated effective joint torque. We formulate this identification problem as a constraint nonlinear optimization problem, which is defined as:

$$\begin{aligned} \underset{\mathbf{CoM}, m}{\operatorname{argmin}} \quad & J = \sum_{i=1}^n \frac{1}{2} [w_1 (\tau_i^1 - f_1(\mathbf{CoM}, m, \mathbf{q}_i))^2 \\ & + w_2 (\tau_i^2 - f_2(\mathbf{CoM}, m, \mathbf{q}_i))^2] \\ \text{subject to:} \quad & \mathbf{CoM}_{min} < \mathbf{CoM} < \mathbf{CoM}_{max} \\ & m > 0 \end{aligned}$$

in which  $w_1$  and  $w_2$  are the weights for costs of two elbow joints.  $\mathbf{CoM}_{min}$  and  $\mathbf{CoM}_{max}$  represent a cuboidal convex hull of the geometry of the object.

Eventually, the CoM location is transformed to the object's body frame based on the known gripping position and orientation of the object.

#### A. Positive Work Direction Searching

For unknown objects, the joint torque can not be derived analytically. So the positive-work directions are detected by



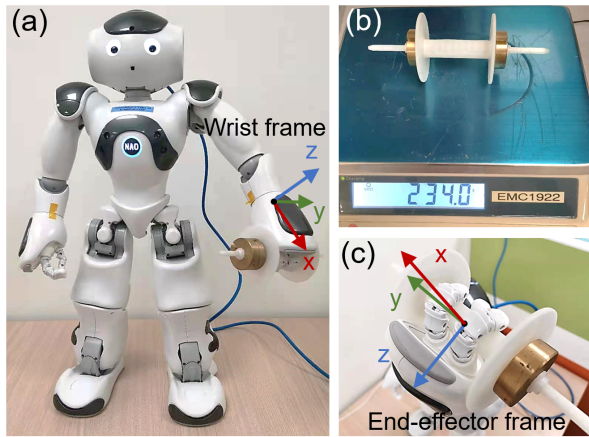


Fig. 5. Experimental setup. (a) Robot holds a dumbbell with known weight firmly during the training experiments. (b) The weight of a sample of a designed dumbbell. (c) A snapshot of the NAO gripping the dumbbell.

experiments. For each joint, we rotate the joint back and forth around the desired configuration, and compare the joint angle errors in steady states which are reached from different directions. The direction with a larger magnitude of joint angle error is marked as positive-work direction. The details are shown in Algorithm 1.

## V. EXPERIMENTS

### A. Experimental Design

The inertial properties of the training objects and testing objects are pre-measured as known inertial properties or ground truth for evaluation. The coordinates of CoM locations are defined in end-effector frame (Fig. 5(c)), whose origin is located at the center of end-effector, and the axes are along the same directions as wrist frame (Fig. 5(a)).

As shown in Fig. 5(a), we design a dumbbell with adjustable weights for the network training experiments. The mass and CoM of the dumbbell can be changed by adjusting the weights on each side (Fig. 5(b)). In the experiments, the robot grips the dumbbell tightly without sliding (Fig. 5(c)). The network training dataset include 13 dumbbells with different masses, which varies from 34 g to 334 g. Since the dumbbell is rotationally symmetrical along y axis in end-effector frame, the x and z components of CoM location are equal to zero. The overall y components of CoM location in the training process range from 0 to -50.7 mm.

3 dumbbells and 3 household tools in Fig. 7(a) are tested to verify the proposed method. The ground truth of physical properties of test objects are shown in Table II. Similar to dumbbells, the screwdriver is rotationally symmetrical. The wrench and pliers are not rotationally symmetrical so both y and z components of their CoM locations are non-zero.

### B. Measurements Processing

In training process, 500 samples of measurements are collected for each pair of dumbbell and configuration. The raw measurements of each joint of the NAO robot are command

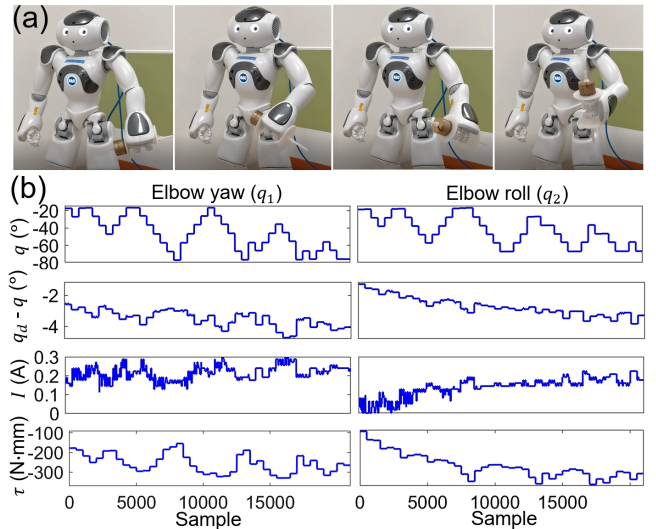


Fig. 6. (a) Snapshots of an example of the training experiments. (b) From the top to the bottom show the joint angle, control steady-state error, electric current and ground truth torque for the elbow yaw (left) and elbow roll (right) relative to the training experiment shown in (a).

joint angle, measured joint angle and electric current. Steady-state joint angle error is obtained by subtracting measured joint angle from command joint angle. Given the inertial properties of objects and the joint angles of the robot, the effective joint torque can be derived analytically .

Fig. 6 shows an example of training experiments. The mass of the dumbbell is 284.0 g and the CoM is (0, -47.1 mm, 0). The sensor measurements and the derived effective joint torques are shown in Fig. 6(b). It is shown that the changing trends of joint angle error and current are in line with that of joint torque. It is observable that joint angle error is more stable and less noisy compared to the electric current.

### C. Neural Network Joint Torque Output Evaluation

The neural network is trained by the dataset collected in the training process. To evaluate the trained neural network, the robot grips different unknown objects and test them in different arm configurations. We compare the output effective joint torque and the reference joint torque derived using the human-measured inertial properties of unknown objects. In addition, the joint torque measurements analytically derived from joint angle steady-state error are also put into comparison. The analytical method is based on the assumption that joint angle steady-state error is proportional to the joint torque (see Section III-A). The coefficients are identified by least squares approximation using the same training dataset as neural network. To explore the effects of components of input, we trained neural networks with different inputs as ablation study. The evaluation metric for joint torque output is defined by mean absolute percentage error (MAPE):

$$e_{\tau} = \frac{1}{n} \sum_{i=1}^n \left| \frac{\hat{\tau}_i - \tau_i}{\tau_i} \right| \times 100\% \quad (7)$$

where  $\hat{\tau}_i$  is the estimated torque,  $\tau_i$  is the reference torque,  $n$  is the amount of estimation results.

TABLE I  
MAPE OF TORQUE ESTIMATION

Input of neural network			Mean absolute percentage error (MAPE) (%)						
$q_d - q$	$I$	$q$	Dumbbell 1	Dumbbell 2	Dumbbell 3	Screwdriver	Wrench	Pliers	Average
✓	✓	✓	6.69	6.10	5.80	10.36	8.70	7.22	7.48
✓		✓	7.35	6.17	5.68	7.80	6.65	10.81	7.41
	✓	✓	12.90	9.99	8.34	24.91	21.88	13.41	15.24
✓	✓		15.64	12.78	15.17	23.96	23.23	15.28	17.68
✓			12.60	12.80	13.25	17.63	17.09	9.41	13.80
	✓		18.37	17.35	16.79	30.40	29.25	16.23	21.40
		✓	19.30	14.44	14.18	32.17	17.57	21.01	19.78
Analytical method by $q_d - q$			21.11	16.25	12.57	49.32	40.56	9.99	24.97

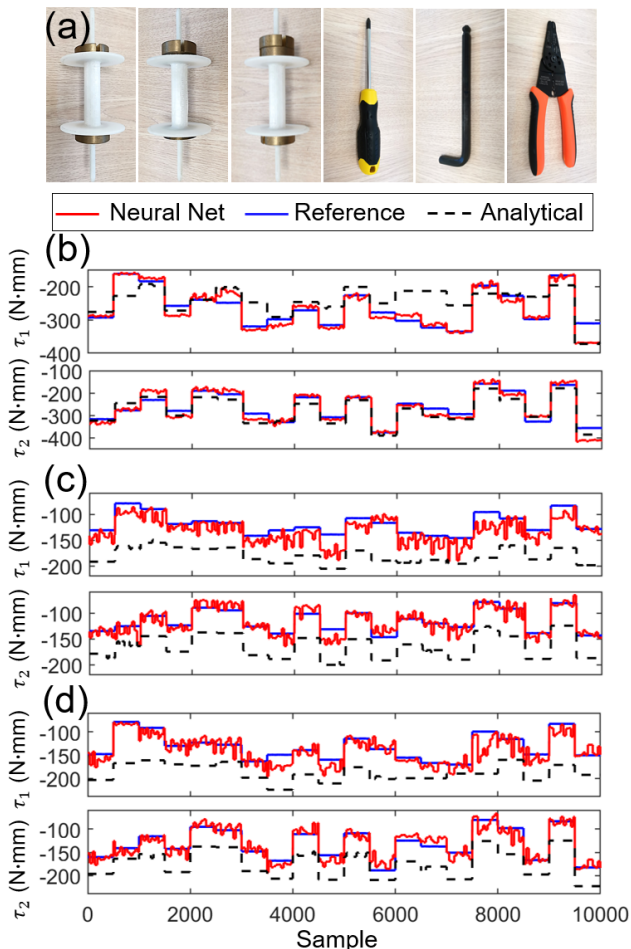


Fig. 7. (a) Snapshots of the testing samples. (b) The reference joint torque (blue), the estimated joint torque by neural network (red), the analytically derived joint torque by joint angle error (black) for the elbow yaw (up) and elbow roll (bottom) for the dumbbell 3 sample. (c) The results of the screwdriver sample. (d) The results of the wrench sample.

The results of joint torque estimation by neural networks with different inputs and analytical method are summarized in Table I. It can be seen that the correlation between joint torques and available measurements are learned by the network. The neural networks perform much better than analytical method. Results also show that the joint angle error

improves the estimation accuracy significantly. The MAPE of the network with only joint angle error and joint angle as input is close to that of the network with all the 3 kinds of inputs. We still substitute the estimated effective joint torques of the network with all kinds of inputs to identification process. Because these results of estimated joint torques incorporate the information from electric current sensors besides the information from encoders.

The joint torque curves during identification process of 3 examples of dumbbell 3, screwdriver and wrench are plotted in Fig. 7(b), (c) and (d) respectively. The estimation results by the neural network although slightly fluctuate but closely follow the reference value.

#### D. Inertial Properties Identification Evaluation

Based on the estimation of joint torques, the mass and CoM location of the unknown object can be obtained via nonlinear optimization. Since dumbbells and screwdriver are rotationally symmetric, the CoM locations of them can be represented by only the y components of CoM. Therefore, during identification process, x and z components of CoM locations are fixed to zero, while y components and masses are identified. The wrench and pliers are not rotationally symmetric, of which both y and z components of CoMs are non-zero. In these cases, x components are fixed to zero, the other 3 parameters (2 for CoM and 1 for mass) are estimated.

We use the following two error metrics to evaluate the results of physical properties identification. The absolute percentage error between estimated mass and ground truth is defined as:

$$e_m = \frac{|\hat{m} - m|}{m} \times 100\% \quad (8)$$

where  $\hat{m}$  is the estimated mass,  $m$  is the reference mass.

The percentage error of CoM is defined as:

$$e_{\text{com}} = \frac{|\hat{r}_{\text{com}} - r_{\text{com}}|}{L_{\text{diag}}} \times 100\% \quad (9)$$

where  $\hat{r}_{\text{com}}$  and  $r_{\text{com}}$  are the coordinates of estimation and ground truth of CoM.  $L_{\text{diag}}$  is the length of the diagonal of the smallest cuboid that can enclose the object.

The results of physical properties identification for unknown objects are shown in Table II. It shows that the CoM estimation error for all the unknown objects are less

TABLE II  
PHYSICAL PROPERTIES IDENTIFICATION

Object	Reference		Estimation		Error metric	
	Mass (g)	CoM (mm)	Mass (g)	CoM (mm)	Mass error (%)	CoM error (%)
Dumbbell 1	234.0	(0, 0, 0)	227.5	(0, -4.7, 0)	2.78	3.02
Dumbbell 2	234.0	(0, -21.6, 0)	246.8	(0, -20.5, 0)	5.47	0.71
Dumbbell 3	334.0	(0, -16.9, 0)	356.2	(0, -10.1, 0)	6.65	4.37
Screwdriver	83.0	(0, -52, 0)	85.7	(0, -67.9, 0)	3.25	7.25
Wrench	125.5	(0, -18.27, 3.5)	121.6	(0, -30.5, 1.3)	3.11	5.58
Pliers	186.5	(0, -41, -24)	179.1	(0, -39.3, -20.1)	3.96	2.31

than 7%; The CoM location estimation error for both 1D (dumbbells and screwdriver) and 2D (srench and pliers) cases are less than 8%. The result shows that our proposed method can obtain relatively accurate estimation without using commercial F/T sensors.

## VI. CONCLUSION

A neural network based framework for estimating inertial properties of unknown objects is proposed in this paper. A MLP is designed to estimate effective joint torques taking joint angle steady-state error, electric current and joint angle as inputs. The mass and CoM location of unknown objects can be identified based on the estimated joint torques from the neural network. By distinguishing different cases of frictional torque due to rotational directions of joints, we develop the planning strategy for both training and testing processes. In this way, the network can be trained with a relatively small dataset. Experiments on NAO robot show that the average percentage error of torque estimation is 7.48% and the physical properties are identified with mass error less than 7% and CoM error less than than 8%. In conclusion, the proposed method can obtain relatively accurate estimation of physical properties of unknown objects without using commercial F/T sensors.

## ACKNOWLEDGMENT

The authors thank Yunshan Ma for the suggestions on neural network and Sipu Ruan for the helpful discussion about experimental setup. Zizhou Lao acknowledges the financial support from NUS Research Scholarship.

## REFERENCES

- [1] C. G. Atkeson, C. H. An, and J. M. Hollerbach, "Rigid body load identification for manipulators," in *24th IEEE Conference on Decision and Control*. IEEE, 1985, pp. 996–1002.
- [2] Y. Yu, K. Fukuda, and S. Tsujio, "Estimation of mass and center of mass of graspless and shape-unknown object," in *Proceedings 1999 IEEE International Conference on Robotics and Automation*, vol. 4. IEEE, 1999, pp. 2893–2898.
- [3] M. T. Mason, "Mechanics and planning of manipulator pushing operations," *The International Journal of Robotics Research*, vol. 5, no. 3, pp. 53–71, 1986.
- [4] T. Yoshikawa and M. Kurisu, "Identification of the center of friction from pushing an object by a mobile robot," in *Proceedings IROS'91: IEEE/RSJ International Workshop on Intelligent Robots and Systems' 91*. IEEE, 1991, pp. 449–454.
- [5] K. M. Lynch and M. T. Mason, "Stable pushing: Mechanics, controllability, and planning," *The international journal of robotics research*, vol. 15, no. 6, pp. 533–556, 1996.
- [6] Y. Han, R. Li, and G. S. Chirikjian, "Can I lift it? humanoid robot reasoning about the feasibility of lifting a heavy box with unknown physical properties," in *2020 IEEE/RSJ International Conference on Intelligent Robots and Systems (IROS)*. IEEE, 2020, pp. 3877–3883.
- [7] C. M. Heunis, V. Belfiore, M. Vendittelli, and S. Misra, "Reconstructing endovascular catheter interaction forces in 3d using multicore optical shape sensors," in *2019 IEEE/RSJ International Conference on Intelligent Robots and Systems (IROS)*. IEEE, 2019, pp. 5419–5425.
- [8] L. Hawley, R. Rahem, and W. Suleiman, "External force observer for small-and medium-sized humanoid robots," *International Journal of Humanoid Robotics*, vol. 16, no. 06, p. 1950030, 2019.
- [9] N. Kofinas, E. Orfanoudakis, and M. G. Lagoudakis, "Complete analytical inverse kinematics for nao," in *2013 13th International Conference on Autonomous Robot Systems*. IEEE, 2013, pp. 1–6.
- [10] C. Wright, A. Johnson, A. Peck, Z. McCord, A. Naaktgeboren, P. Gianfortoni, M. Gonzalez-Rivero, R. Hatton, and H. Choset, "Design of a modular snake robot," in *2007 IEEE/RSJ International Conference on Intelligent Robots and Systems*. IEEE, 2007, pp. 2609–2614.
- [11] R. W. Hogg, A. L. Rankin, S. I. Roumeliotis, M. C. McHenry, D. M. Helmick, C. F. Bergh, and L. Matthies, "Algorithms and sensors for small robot path following," in *Proceedings 2002 IEEE International Conference on Robotics and Automation*, vol. 4. IEEE, 2002, pp. 3850–3857.
- [12] D. Gouaillier, V. Hugel, P. Blazevic, C. Kilner, J. Monceaux, P. Lafourcade, B. Marnier, J. Serre, and B. Maisonnier, "Mechatronic design of nao humanoid," in *2009 IEEE International Conference on Robotics and Automation*. IEEE, 2009, pp. 769–774.
- [13] A. C. Smith and K. Hashtrudi-Zaad, "Application of neural networks in inverse dynamics based contact force estimation," in *Proceedings of 2005 IEEE Conference on Control Applications*. IEEE, 2005, pp. 1021–1026.
- [14] N. Yilmaz, J. Y. Wu, P. Kazanzides, and U. Tumerdem, "Neural network based inverse dynamics identification and external force estimation on the da vinci research kit," in *2020 IEEE International Conference on Robotics and Automation (ICRA)*. IEEE, 2020, pp. 1387–1393.
- [15] A. Marban, V. Srinivasan, W. Samek, J. Fernández, and A. Casals, "A recurrent convolutional neural network approach for sensorless force estimation in robotic surgery," *Biomedical Signal Processing and Control*, vol. 50, pp. 134–150, 2019.
- [16] T. Mattioli and M. Vendittelli, "Interaction force reconstruction for humanoid robots," *IEEE Robotics and Automation Letters*, vol. 2, no. 1, pp. 282–289, 2016.
- [17] W. Hwang and S.-C. Lim, "Inferring interaction force from visual information without using physical force sensors," *Sensors*, vol. 17, no. 11, p. 2455, 2017.
- [18] D. Kim, H. Cho, H. Shin, S.-C. Lim, and W. Hwang, "An efficient three-dimensional convolutional neural network for inferring physical interaction force from video," *Sensors*, vol. 19, no. 16, p. 3579, 2019.
- [19] J. A. Heredia and W. Yu, "A high-gain observer-based pd control for robot manipulator," in *Proceedings of the 2000 American control conference. ACC*, vol. 4. IEEE, 2000, pp. 2518–2522.
- [20] D. W. Robinson, J. E. Pratt, D. J. Paluska, and G. A. Pratt, "Series elastic actuator development for a biomimetic walking robot," in *1999 IEEE/ASME International Conference on Advanced Intelligent Mechatronics*. IEEE, 1999, pp. 561–568.